APPLIED MEASUREMENT SYSTEMS

Edited by **Md. Zahurul Haq**

INTECHWEB.ORG

Applied Measurement Systems
Edited by Md. Zahurul Haq

Published by InTech
Janeza Trdine 9, 51000 Rijeka, Croatia

Publishing Process Manager Mirna Cvijic
Technical Editor Teodora Smiljanic
Cover Designer InTech Design Team

First published February, 2012
Printed in Croatia

A free online edition of this book is available at www.intechopen.com
Additional hard copies can be obtained from orders@intechweb.org

Applied Measurement Systems, Edited by Md. Zahurul Haq
p. cm.
ISBN 978-953-51-0103-1

Contents

2

Internal Combustion Engine Indicating Measurements

André V. Bueno[1], José A. Velásquez[2] and Luiz F. Milanez[3]
[1]*Federal University of Ceara, UFC,*
[2]*Federal University of Technology - Parana, UTFPR,*
[3]*University of Campinas, UNICAMP,*
Brazil

1. Introduction

Engine indicating includes the measurement of instantaneous in-cylinder pressure, the determination of the top dead centre (TDC) and the measurement of the instantaneous crank angle (c.a.). These measurements are fundamental for engine combustion diagnosis and for indicated work calculation.

In engine combustion diagnosis, the apparent heat release rate and the combustion reaction extent are the most useful quantities obtainable from engine indicating data. The apparent heat release rate is calculated by computing the amount of fuel chemical energy release necessary to obtain the experimentally observed pressure, while the combustion reaction extent is evaluated through the released fraction of the total fuel chemical energy. Heat release analysis is often complemented using optical techniques and its utilization as a diagnostic tool covers a wide range of objectives, including the development of new combustion systems, the analysis of alternative fuel burning, the validation of mathematical models for engine simulation, the investigation of combustion chamber insulation effects and the study of new injection strategies.

Taking into account the importance of indicating measurements for engine research and development, this chapter addresses the description of a modern engine indicating measurement system and includes recommendations about good-practice procedures and cares that a researcher must observe in order to perform accurate experiments and to obtain valuable information from measured data.

1.1 A word on the evolution of engine indicating measurement systems

The measurement of the working fluid pressure of heat engines was a topic of interest for engineers since the advent of the steam engine, for which the Watt's indicator was developed. When the internal combustion engine became the most widespread heat machine, its analyses and improvements also demanded the measuring of in-cylinder pressure data and early measurements were accomplished utilizing several configurations of mechanical indicators (Amann, 1985). However, as the operating speeds increased with

the development of the engines, the frequency response of such mechanical indicators became deficient, making them obsolete in the mid-sixties of the last century.

High-speed electronic transducers, capable of converting the deflection of a low inertia diaphragm into an electrical signal were designed to meet the demand for pressure measuring instruments with superior characteristics. Early versions of such devices already had adequate frequency response to the phenomena occurring in the engine combustion chamber, having been built using extensometers (Draper & Li, 1949) and piezoelectric crystals (Kistler, 1956) as sensing elements. Nevertheless, these new electronic pressure transducers were initially coupled to analog data acquisition systems made of a signal conditioning amplifier, a cathode-ray oscilloscope and a photo camera that was used to record the pressure signal from the oscilloscope screen (Brown, 1967). This data generating procedure was cumbersome and had a number of uncertainties related to the film exposure time as well as to the oscilloscope trace (Benson & Pick, 1974).

At the end of the 1960s, complex analog systems capable of carrying out a fully electronic processing of the transducer signal became available. These devices were firstly used for specific applications, such as determining the indicated power (Alyea, 1969), indicated mean effective pressure (Brown, 1973), as well as studying knock and misfire in spark ignition engines (Alwood et al., 1970). The user interface was through a voltmeter, which displayed a voltage proportional to the indicated mean effective pressure or, alternatively, by means of an electromechanical counter that showed the number of cycles in which knock or misfire occurred.

In the mid-seventies, when analog-to-digital converters were included in the instrumentation, multipurpose and of-less-complexity experimental sets became available (Benson & Pick, 1974; Ficher & Macey, 1975; Marzouk & Watson, 1976). From this time, the signal from instrumentation amplifiers has been digitalized and stored in a computer, allowing further manipulation via software. Therefore, greater storage capacity and flexibility in data analysis were assured, maintaining an acceptable level of accuracy.

Nowadays these are typical characteristics of a modern engine indicating system, as the one schematically represented in Figure 1, which includes components suitable for measurements in diesel engines. In this scheme, the fuel injection line pressure is measured with a strain-gauge based sensor connected to an instrumentation amplifier, while the signal generated by a piezoelectric pressure sensor can be conditioned following two measurement procedures, which are addressed in detail in the present chapter. In the first procedure, the in-cylinder pressure is obtained by employing a charge amplifier for conditioning the transducer signal, while in the second procedure a current-to-voltage converter is used to measure the in-cylinder pressure derivative.

Pressure data are indexed with the angle position of the crankshaft, with reference to the compression TDC. Usually the crankshaft angle position is determined with an optical angle encoder, which provides both — one pulse per revolution in a channel used to establish the TDC angle reference, and 720 pulses per revolution in a second channel to determinate the instantaneous relative angle position. External pulse multipliers may also be available to improve the relative angle position resolution up to 3600 pulses per revolution. Each angle position pulse triggers a high speed data acquisition system, which should be able to simultaneously acquire the signals provided by the conditioning amplifiers, collect the acquired data among multiple cycles for cycle averaging, and save it in a storage computer.

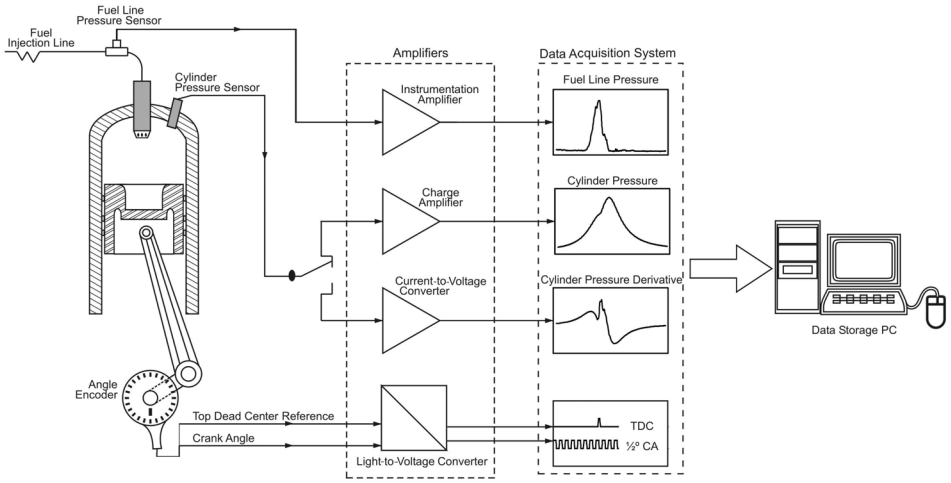

Fig. 1. A typical engine indicating measurement system.

2. The transducer for in-cylinder pressure measurement

The analysis of the processes occurring in the cylinder of internal combustion engines requires pressure transducers with high specifications regarding linearity, frequency response and resistance to thermal solicitations. Studies comparing transducers available at the end of 1960 decade (see for example Brown, 1967) found that those having piezoelectric crystals as measuring elements exhibited better tolerance to thermal solicitations than those based on strain gauges. By this reason, piezoelectric transducers eventually spread to measure the in-cylinder pressure, while sensors based on strain gauges (metal or piezo-resistive) were preferably used in measurements where the thermal solicitations are modest, such as pressure measuring in the fuel injection line and in the intake manifold.

Piezoelectric transducers are capable of maintaining high characteristics in frequency response and linearity over a wide range of pressures. On the other hand, the main reported drawbacks to their use include instability of the baseline and low intensity of its output signal. These drawbacks and their control will be discussed in Section 2.4, where the techniques for conditioning the pressure transducer signal will be presented.

2.1 Operating principle of the piezoelectric pressure transducer

Figure 2 illustrates the principle of operation of a piezoelectric pressure transducer. The pressure change rate (dP/dt) experienced by the transducer diaphragm is transmitted to a piezoelectric crystal through intermediate elements, causing its deformation at a rate $d\varepsilon/dt$.

Due to the piezoelectric effect, this deformation polarizes charge q in the transducer electrode originating an electric current i, which constitutes the transducer output signal:

$$i = -\frac{dq}{dt} = -G_s \frac{dP}{dt} \tag{1}$$

where G_s is the transducer sensitivity (gain).

During the measurement of in-cylinder pressure, the transducer is exposed to a transient heat flow that causes continuous changes in its temperature. These temperature changes modify the sensitivity of the piezoelectric element and impose thermal stresses in the diaphragm and in the sensor housing, generating spurious forces that act on the quartz element and cause additional distortion of the signal provided by the transducer. The inaccuracy due to these effects receives the name of temperature drift (Marzouk & Watson, 1976).

It is usual to separate the temperature drift into two components. The first one corresponds to changes in heat flow that occur within each cycle, and is named short-term drift or thermal shock. The second component represents the slow change in the transducer temperature resulting from variations in the engine operating conditions and is known as load-change drift or long-term drift.

Normally, the long-term drift only promotes a slow instability in the baseline for transducer signal, whose consequences and control depend on the circuitry chosen for its polarization.

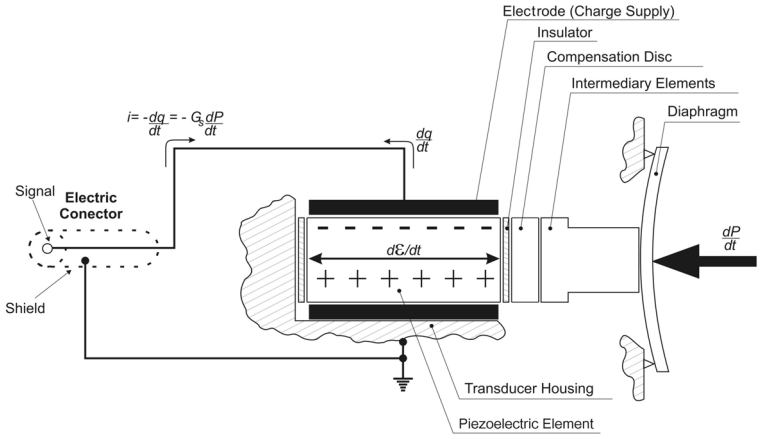

Fig. 2. The piezoelectric pressure transducer.

The effects of the short-term drift, in turn, depend on the intensity with which this phenomenon occurs. A severe short-term, such as that resulting from operating conditions that can permanently damage the transducer, may produce pressure values below the atmospheric pressure at the end of the expansion process. At more restrained levels, however, the presence of short-term drift cannot be readily identified, causing the pressure reading to be higher than the actual in-cylinder pressure during combustion, and lower throughout the remainder of the expansion. Although modern piezoelectric sensors are designed to minimize the effects of short-term drift, it must be taken into account that the intensity of the latter strongly depends on the thermal load at the transducer location. This thermal load is influenced by the intense flows during the gas exchange process, by the approximation of the fuel jet in a diesel engine or by the flame front approximation in a spark-ignition engine. Thus, checking the extent of the thermal shock at the transducer location in each particular case is a good practice for an accurate measuring.

2.2 Choice of the transducer mounting location

The installation of the piezoelectric pressure transducer must be preceded by the calibration of the complete measuring chain formed of the piezoelectric transducer, the signal conditioning amplifier and the data acquisition system. It is possible to use a dead-weight calibrator for this task in accordance with the recommendations made by Lancaster et al. (1975). The choice of the location where the transducer will be mounted should prioritize well-cooled regions of the head and avoid these where thermal stresses can induce deformations in the transducer housing. The diaphragm of the sensor should be positioned as recommended by the manufacturer (usually, with a gap of 1.5 to 3.0 mm from the inner surface of the head). Water-cooled transducers feature superior gain (higher signal/noise ratio), linearity and thermal resistance respective to the miniature uncooled transducers, and should be the first choice for use in cases where there is enough space in the head. Channels connecting the combustion chamber with the cavity where the sensor diaphragm is located may behave as acoustic resonators, generating pressure oscillations and their consequent measurement inaccuracies, which can invalidate the evaluation of both, the indicated thermodynamic parameters and the combustion energy release. So, the use of these channels (as typically occurs when the sensor is embedded in a spark plug) is recommended only for the identification of abnormal combustion in spark ignition engines.

In-cylinder pressure measurements in direct injection (DI) diesel engines demand extra care due to the high compression ratio and to the shape of the combustion chamber. In these engines, when the piston is near the TDC, about 90% of the working fluid mass is inside the piston bowl and in the region above this cavity. The pressure of this mass portion is representative of the cylinder averaged pressure. The remaining mass occupies the crevice regions between piston and head as well between piston and sleeve, and its pressure may exhibit oscillations of up 10 bar amplitude, which are due to the turbulent in-cylinder flow and to acoustic phenomena resulting from combustion. Thus, the transducer must be located at a point from which the pressure of the mass above the piston bowl can be accessed. Finally, it is important to point out that when choosing the transducer mounting point the fuel jet impingement on the transducer diaphragm should also be avoided.

2.3 Validation of the transducer mounting location

In order to illustrate the procedure for validating the transducer mounting location we will consider as example the case of a fast, direct injection diesel engine with three valves per cylinder, in which indicating measurements were conducted using an uncooled mini-transducer AVL GM 12 D, mounted above the piston bowl in the glow plug place, as shown in Figure 3.

The method proposed by Randolph (1990) allows checking the occurrence of short-term drift by comparing the cycle-to-cycle variability of the in-cylinder pressure readings at specified instants along the working cycle. Certain variability is normal due to the random nature of the combustion process, which causes one cycle to be slightly different from other under unchanged operating conditions. This cycle-to-cycle variability leads to changes in the thermal load acting on the transducer and, when short-term drift occurs, it leads also to changes in transducer sensibility, thus enlarging the scattering of pressure readings.

In order to apply the Randolph test, consider two points along the cycle, designated as C1 and B2. The first point is the beginning of the exhaust process, thus characterizing a moment when the transducer is under the influence of combustion thermal loads. The second point is located in the compression stroke, thus soon after the gas exchange, during which the transducer is cooled. So, if short-term drift was occurring, it should produce pressure readings at C1 more scattered than those at B2 (Randolph, 1990; Roth el al., 2001). Figure 4 shows the pressure deviations from the sample mean-value, for 56 consecutive cycles. According to the description given above, the short-term drift would cause the scattering of points along the x-axis be greater than that along the y-axis. However, the points in this figure are distributed equitably with respect to the axes, thus implying that short-term drift is trivial in this case. The scattering of points with respect to the diagonal of the graph allows judging about the repeatability of the experiment. The behaviour observed in Figure 4 attests for a good repeatability and is similar to that reported by Roth et al. (2001) for transducers akin to the one used in this example.

Fig. 3. Pressure transducer mounting location.

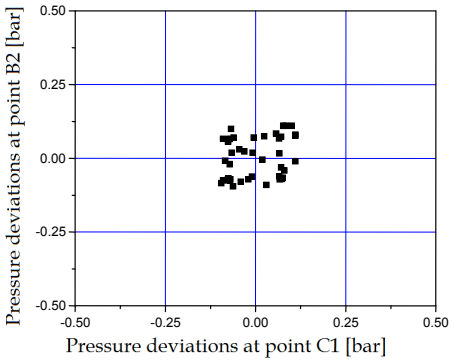

Fig. 4. Deviation of pressure readings respective to sample mean-value. Point C1: 145 c.a. degrees after compression TDC. Point B2: 80 c.a. degrees before compression TDC.

In cases of significant short-term drift, it is recommendable to mount the transducer via an adapter, which avoids its direct contact with the cylinder gas, thus eliminating local heating of the transducer components and, mainly, of its diaphragm. Another solution consists in installing the transducer recessed by means of a measuring channel. However, such mounting procedure may lead to inaccuracies caused by an oscillating flow in the channel. The extent of such inaccuracies has been studied in detail by Hountalas & Anestis (1998).

2.4 Strategies for processing the piezoelectric transducer signal

The strong influence of the pressure derivative on the energy release rate was recognized by several authors (Marzouk & Watson, 1976; Woschni, 1965; Krieger & Borman, 1966). Despite this, indicating measurements usually aim obtaining the in-cylinder pressure, even when combustion diagnosis is the major objective. As a rule, this task is carried out using a piezoelectric transducer polarized by a charge amplifier (Brown, 1976; Marzouk & Watson, 1976; Benson & Pick, 1974; Lancaster et al., 1975; Lapuerta et al., 2000; Benson & Whitehouse, 1983). The preference for this practice can be attributed to the legacy of the mechanical indicators, which were created especially for pressure measuring, as well as to the importance of knowing the in-cylinder pressure for calculating the indicated work or for characterizing the thermodynamic state of the working fluid. Thus, obtaining pressure derivative data for heat release analysis was eventually relegated to the numerical manipulation of available pressure data. As it will be discussed below, this procedure amplifies the inaccuracies in the pressure data, originating pressure derivative curves with oscillations that are eventually transferred to the results of energy release rate calculation.

The numerical instabilities inherent to the differentiation operation motivated the development of experimental arrangements in which this operation was carried out by means of electronic circuits. A reference to such an approach can be found in the work of Marzouk & Watson (1976) who processed the analog signal from a charge amplifier by an electronic differentiator. While avoiding the numerical differentiation of pressure data, these authors did not obtain satisfactory results for the pressure variation rate, underestimating its peak value during the premixed combustion. This was due to the deficient frequency response of the adopted differentiation circuit, which severely damaged the performance processing of those data that make up the high frequencies region of the spectral distribution (see Section 4).

The drawbacks mentioned above can be overcome by employing an alternative technique of polarization of the piezoelectric sensor — the direct conversion of the current signal supplied by the transducer into an analog voltage level proportional to the time rate of change of the in-cylinder pressure. The circuitry presented in Section 2.4.2 is based on this technique.

2.4.1 Signal processing with a charge amplifier

Figure 5 shows a simplified schematic of the experimental setup commonly used to obtain in-cylinder pressure data. A shielded cable with high insulation resistance conducts the charges polarized by the transducer to the inlet of the charge amplifier. This device is based on an integrator circuit, which provides an output voltage proportional to the time integration of the electric current applied at its input during a time interval Δt, taken from

the instant at which it was started (or reset) until the desired instant of measurement. Thus, the pressure variation during the interval Δt is given by

$$\left(P - P_{ref}\right) = \frac{v_{ch} \cdot G_a}{G_s} \tag{2}$$

where P and P_{ref} are values of the pressure acting on the transducer diaphragm at the end and at the beginning of the time interval Δt, respectively; G_a is the gain of the charge amplifier and v_{ch} is the charge amplifier output voltage.

Since the charge produced by the pressure transducer is pretty small, reaching just tens of picocoulombs per bar, the association between a piezoelectric transducer and a charge amplifier results extremely sensitive to non-idealities of electronic circuits, mainly to current leakages occurring through the insulation resistance of the measurement system or even within the integrator circuit. Such current leakages cause a slow and steady decline in the level of the output voltage of the charge amplifier, thus yielding pressure values lesser than the actual ones. In order to control this inaccuracy it is necessary to have high input impedance in the charge amplifier, while taking especial care for maintaining the electrical contacts clean and for operating the data conditioning system in a low-humidity environment.

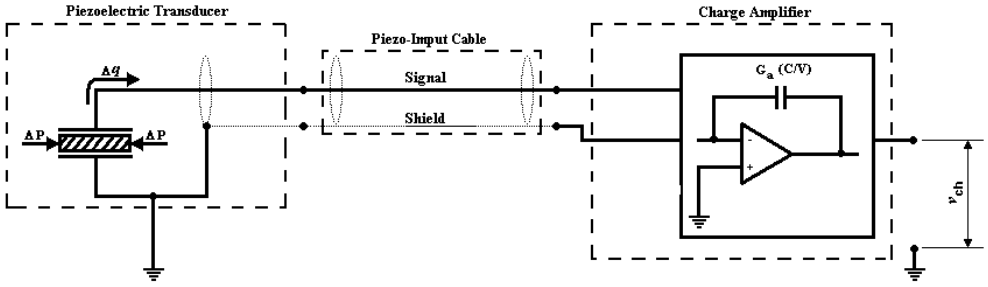

Fig. 5. Transducer signal conditioning through a charge amplifier.

Long-term drift also promotes an incessant and slow displacement of the data baseline as the integrator circuit processes spurious current induced by changes in the transducer temperature, which in its turn result from changes in engine operation conditions.

Therefore, even when properly using a good-quality measuring system, the combined action of circuitry non-idealities and long-term drift leads to instability of the pressure baseline, which is a drawback inherent to the use of a charge amplifier and is reported in the literature as pressure baseline floating (Marzouk & Watson, 1976; Benson & Pick, 1974; Lancaster et al., 1975; Benson & Whitehouse, 1983). This baseline floating can produce pressure deviations of tens of bars during a long-duration measurement, making it mandatory to reset periodically the amplifier in order to avoid its saturation.

The deviations mentioned above as well the fact that pressure data provided by a charge amplifier are related to an initial measurement time make it necessary to correct the baseline at each cycle, as well as the pressure readings. This task can be accomplished by

determining the pressure baseline that leads to a null value of the apparent heat release rate over the first 80 c.a. degrees after the intake valve closing. This criterion for correcting the pressure readings is based on the recommendations given by Lapuerta et al. (2000).

2.4.2 Signal processing with a current-to-voltage converter

The most evident experimental setup for converting the current polarized by a piezoelectric transducer consists in conducting it to the ground through an electrical resistance, thus originating a voltage drop equal to the product of the value of this resistance by the current. Such procedure would result, however, in the formation of an RC circuit between the transducer inherent capacitance and the measurement resistance, which, in turn, would cause attenuation in the voltage drop and a phase delay with respect to the polarized current. In order to avoid this problem Bueno et al. (2009, 2010, 2011) proposed to use a circuit that converts current into voltage (Franco, 2001), consisting of an operational amplifier and a negative feedback resistor, as shown in Figure 6. This circuit operates stably in a range of gains typical for engine indicating measurements, and may undergo minor changes related to balancing techniques, depending of which operational amplifier was chosen for its construction. The virtually zero value of the input impedance of the current-to-voltage converter, given by the ratio of R_A and the open-loop gain of the operational amplifier A_1, makes it immune to inaccuracies arising from the inherent capacitance of the piezoelectric transducer. Besides that, in order to isolate the converter with respect to the impedance of the instrument to which it is connected, a voltage follower amplifier was used. Thus, the pressure rate of change *dP/dt* is given by:

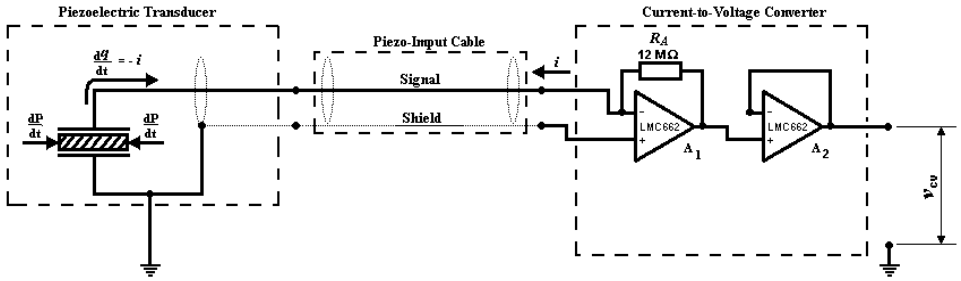

Fig. 6. Transducer signal conditioning through a current-to-voltage converter.

$$\frac{dP}{dt} = \frac{v_{cv}}{G_s \cdot R_A} \tag{3}$$

where v_{cv} is the output voltage of the current-to-voltage converter and R_A is the gain adjusting resistance of the current-to-voltage converter. Taking the crankshaft angle speed as a constant, the following expression for the pressure derivative with respect to crank angle can be obtained:

$$\frac{dP}{d\theta} = \frac{v_{cv}}{6 \cdot G_s \cdot R_A \cdot RPM} \tag{4}$$

in this equation *RPM* represents the engine operating speed, in revolutions per minute.

The in-cylinder pressure can be determined by numerically integrating the data obtained for its derivative. A fourth order Runge-Kutta algorithm is recommended for this task (Teukolsky, 1996) and the pressure baseline can be determined by applying the same correction technique recommended in Section 2.4.1.

The use of a current-to-voltage converter eliminates the need of special care for insulation resistance and leakage currents, as in this case the charges polarized by the transducer unrestrictedly flow to the ground. In addition, the long-term drift makes the pressure derivative baseline to deviate from its original position returning, however, after the engine reaches a steady state. Therefore, this technique also eliminates the need for resetting the transducer polarization circuit due to the large displacements of the data baseline. Further details involving the conditioning of the pressure derivative signal using a current-to-voltage converter can be found in references Bueno et al. (2009) and Bueno et al. (2011).

3. Crank angle measurements and TDC position identification

In modern engine indicating systems the instantaneous position of the crankshaft is determined with the aid of an optical angular encoder, whose operating principle is based on photoelectric scanning of a sequence of thin opaque lines. These lines are etched on a transparent disk that rotates together with the crankshaft and are arranged in the radial direction at equal angular intervals, forming the so-named incremental track (see Figure 7).

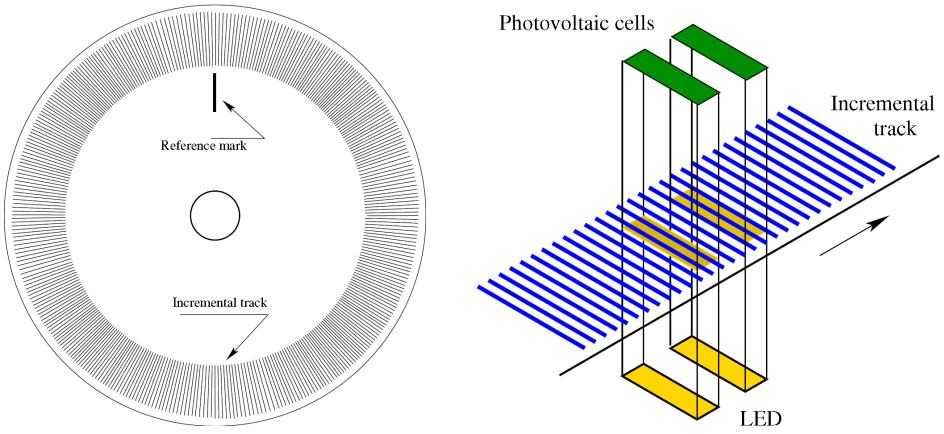

Fig. 7. The optical angle encoder.

During operation of the optical angular encoder a light beam emitted by a LED falls perpendicular to the disk plane on the incremental track. As the disk is rotating, this light beam will be reflected if meets one of the etched lines, but it will pass across the disk while falling on the gap between two lines. Then, a sequence of light pulses synchronized with the crankshaft angular position will pass across the disk and will be conducted through an optical fiber to a light-pulse converter, where photovoltaic cells transform this light signal into an electrical one. Therefore, the encoder outputs a pulse string in response to the amount of rotational displacement of the crankshaft. A separate counter counts the number of output pulses to determine the crankshaft angle position.

In engine indicating measurements the angular position of the crankshaft must be determined in relation to a reference, which is generally also used as reference to identify the position of the TDC. Such reference is generated with the aid of a second incremental track that has a single mark, which is used to reset the counting of the pulses.

Special attention should be given to the correct identification of the TDC position, as small errors in this measurement lead to significant errors in the evaluation of indicated work as well as combustion heat release rate (Krieger & Borman, 1966; Pischinger & Glaser, 1985; Lapuerta et al., 2000). In order to achieve adequate precision in determining the TDC position it is recommended to perform a dynamic measurement, running the engine motored and unfired or, alternatively, preventing combustion only in the cylinder where the measurement is going on, while the other cylinders function fired to keep the engine running.

When performing dynamic measurement, the inaccuracies that would be generated by the bearing clearances are eliminated. Such measurement is usually carried out with a capacitive proximity sensor, or in the absence of such a sensor, the TDC position can be inferred from the motored-engine pressure data.

The capacitive proximity sensor uses two conductive objects separated by a dielectric material. A voltage difference applied to the conductive objects generates an imbalance of electrical charges between them, originating an electric field in the dielectric material. When this voltage is alternated the electrical charges move continuously, going from one of the conductive objects to the other and generating an alternating electric current, which is the output signal of the sensor. The amount of current flow is determined by the capacitance, and the capacitance depends on the proximity of the conductive objects. Closer objects cause greater current than more distant ones.

In the capacitive sensors used to determine the TDC position, one of the conductive objects is the sensor probe itself, while the piston plays the role of the second conductive object (Figure 8). The sensor is mounted in the head in such a way that when the engine is running the piston will move closer or away from the sensor, but without actually touching it. Thus, the sensor will produce a signal with amplitude, which is inversely proportional to the distance between the TDC sensor tip and the piston top. The exact TDC position will correspond to the maximum amplitude of the TDC sensor signal, which can be determined with great accuracy because of the high degree of symmetry of the signal.

When using the motored-engine pressure data for identifying the TDC position, the main arising difficulty is that the peak pressure precedes the actual TDC position, which corresponds to the minimum volume. This occurs due to heat transfer and mass losses, and the angle interval between these events is named loss angle (Figure 9). Several enough accurate methods have been proposed for determining the loss angle (Pinchon, 1984; Stas, 1996), and usually manufacturers of indicating equipment include in their manual recommendations to estimate loss angle values, which depend on the kind of the engine (spark ignition or diesel) and compression ratio.

The advantage of the direct measurement of TDC position, compared with its determination from the motored-engine pressure curve, is that there is no need for a correction involving the loss angle, which always increases the uncertainty.

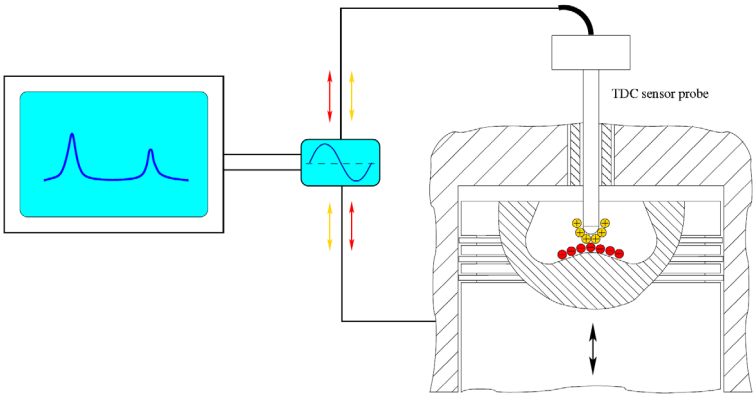

Fig. 8. The capacitive TDC sensor.

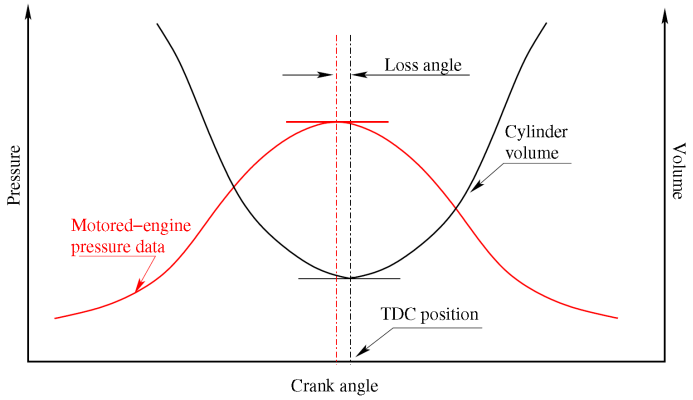

Fig. 9. Definition of loss angle.

4. Uncertainty sources and data treatment

Cylinder pressure data measured by a transducer can be understood as being the sum of two components: *(i)* a smooth component, corresponding to the instantaneous average pressure through the entire cylinder volume; and *(ii)* a spurious component, originated by both the turbulent flow of gas inside the cylinder and the acoustic pulsations associated to combustion. According to the hypothesis of the single-zone combustion model (Krieger & Borman, 1966), the first component must be used to characterize the thermodynamic state of the gases in the cylinder, constituting the information of interest for heat release analysis. The second component is small when compared to the first one and its extent is influenced by the transducer mounting location in the combustion chamber. In addition to these two components of the measured pressure, the experimental data also include noise generated by the measurement system during the conditioning of the transducer output signal. Thus, for accurate heat release analysis it is necessary to isolate the volume-averaged pressure component from both the flow and the combustion driven spurious component as well as from the measurement noise.

Typically, the assessment of the smooth volume-averaged pressure component has been accomplished by means of numerical treatment of experimental data, which is usually carried out after data averaging over several consecutive cycles. A diversity of methods can be used for this numerical treatment, including FFT filters, windowing filters, smoothing splines and Wiebe function regression (Zhong et al., 2004; Payri et al., 2011; Ding et al., 2011). However, the choice of a proper data treatment methodology requires, at least, a basic knowledge about the behaviour of each one of the above mentioned components of the experimental data. In order to assess this behaviour Bueno et al. (2009) proposed to estimate the smooth component corresponding to the average pressure through the entire cylinder volume and, then, to employ it to analyze the spurious component of the experimental data. Sections 4.1 through 4.3 show how this task is accomplished.

4.1 The volume-averaged smooth data component

Smooth component curves (referred here as *reference curves*) for both in-cylinder pressure and in-cylinder pressure derivative data can be estimated by means of a computer routine based on the single-zone combustion model. In this routine, the combustion heat release rate is modelled through Wiebe functions (Wiebe, 1970) whose adjusting constants are obtained by optimizing curve-fitting to heat release rate data calculated from measured values. Figure 10 shows typical reference curves and experimental data obtained with each one of the signal conditioning procedures described in Sections 2.4.1 and 2.4.2. The curves shown in Figure 10 are related to a direct injection diesel engine and they show that the premixed burning causes a steep slope in the pressure curve region subsequent to ignition (circled area in Figure 10a), whilst in the pressure derivative curve it is reflected as a prominent peak (circled area in Figure 10b). By comparing these two representations, it becomes evident that the premixed combustion is more visible in the pressure derivative curve, a fact that led to the choice of the pressure derivative as the basic representation for the analysis of the data given by the indicator system.

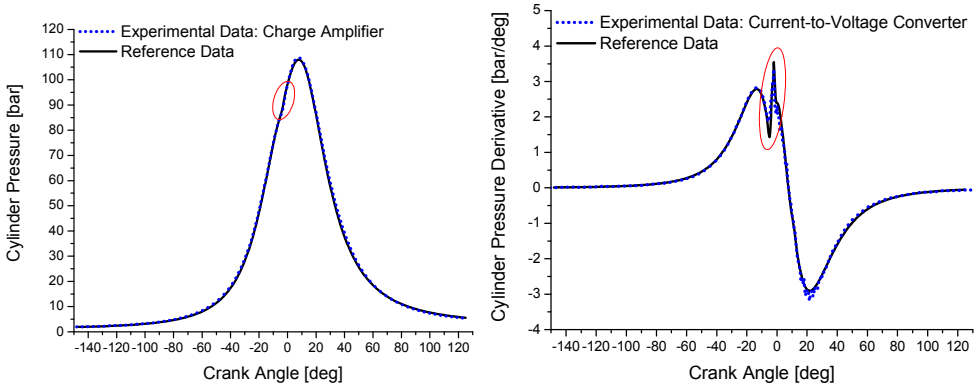

(a) (b)

Fig. 10. Typical reference curves for pressure and pressure derivative data (D.I. diesel engine running at 2600 rpm and 80% of full load).

Frequency domain representations such as Lomb periodograms (Lomb, 1976) constitute a suitable tool for the analysis of experimental data. In these periodograms the spectral power is normalized with respect to the variance of the analyzed data, and its value represents the degree of participation of the signal associated to a given frequency in the data composition. In Figure 11, spectral distributions of two pressure derivative curves obtained through numerical simulation are compared. The first curve, named *Reference Data*, was calculated using two Wiebe functions, corresponding to premixed and diffusive stages of combustion, respectively. The second curve, named *Diffusive Combustion Data*, was obtained suppressing the premixed combustion and only one Wiebe function representing diffusive combustion was used. As can be seen in Figure 11, these curves exhibit similar spectral power distribution in the low-frequency region (up to 1000 Hz); however, in the region between 1000 and 5000 Hz the suppression of premixed combustion caused considerable attenuation of the pressure derivative data. Thus, it may be concluded that the contribution of the premixed combustion is located in this frequency range (from 1000 to 5000 Hz) and that the utilization of low-pass filters or numerical treatment to smooth the transducer signal at frequencies below 5000 Hz may cause distortion or even the elimination of the influence of premixed combustion on experimental data. It may also be observed that the effects of both the compression process and the diffusive combustion play a major role in the spectral distribution of the data of interest, occupying the frequency range with highest spectral power values (below 1000 Hz).

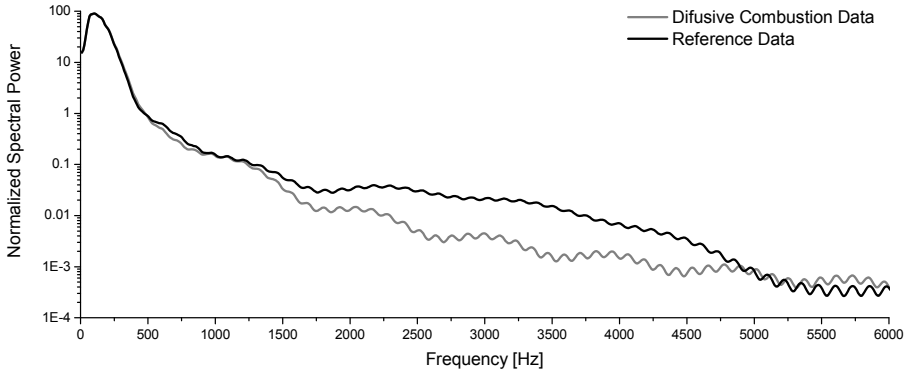

Fig. 11. Spectral distribution for simulated in-cylinder pressure derivative data (D.I. diesel engine running at 2600 rpm and 80% of full load).

4.2 Measurement system noise and the flow driven spurious component

Uncertainties associated to the data acquisition system are dominated by the truncation error of the analog-to-digital converter, acting as a source of white noise in the acquired experimental signal. Therefore, the measurement uncertainty due to this noise (*MU*) can be estimated in terms of the analog-to-digital converter accuracy, which corresponds to the least-significant bit (*LSB*) of the used measurement system.

When a transducer is polarized by a charge amplifier, the influence of this uncertainty on the pressure derivative curve is indirect, because the measured parameter in this case is the in-cylinder pressure. Nevertheless, it is possible to estimate the measurement uncertainty

imposed by the quantization noise to the pressure derivative (MU_{dP}) using finite differences approximation of fourth order. Doing so and taking into account that data reported in Figures 10 and 11 refer to measurements made with a system whose *LSB* value is 0.131 bar, results

$$MU_{dP} = \pm\sqrt{\left(\left(\frac{LSB}{12\Delta\theta}\right)^2 + \left(\frac{-8LSB}{12\Delta\theta}\right)^2 + \left(\frac{8LSB}{12\Delta\theta}\right)^2 + \left(\frac{-LSB}{12\Delta\theta}\right)^2\right)} = \pm 0.25 \ \textbf{bar/}\deg \tag{5}$$

On the other hand, when the direct polarization of the transducer is used, the pressure derivative is accessed directly and the measurement uncertainty imposed by the quantization noise to the pressure derivative is given by the corresponding *LSB* value. In the case of the data reported in Figures 10 and 11 this value is 54.694 bar/s, then

$$MU_{dP} = \pm\ 54.694 \ \textbf{bar/s} = \pm 3.5 \times 10^{-3} \ \textbf{bar} / \deg \tag{6}$$

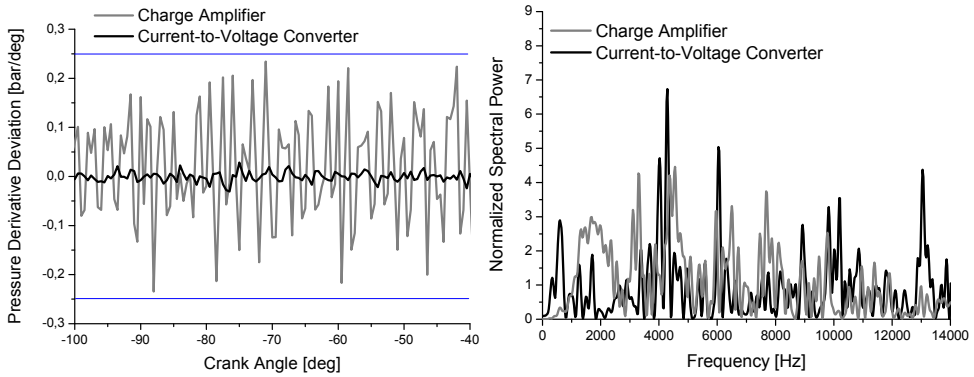

(a) (b)

Fig. 12. Deviations due to the measurement system noise and to the in-cylinder flow (D.I. diesel engine running at 2600 rpm and 80% of full load).

It must be noticed that the utilization of a current-to-voltage converter allowed reducing the measurement uncertainty imposed by the quantization noise to only 1.4% of the value obtained using a charge amplifier. As it will be discussed later, this fact has important consequences for obtaining smooth heat release rate diagrams. Additionally, when signal conditioning is carried out using a charge amplifier, the refinement of the encoder resolution increases the measurement uncertainty, whilst for the case of the current-to-voltage converter the measurement uncertainty does not depend on the encoder resolution.

Figure 12a shows experimental data deviation from the reference pressure derivative curve during the compression process, when combustion does not occur and, therefore, the spurious components of the experimental data can be attributed only to the in-cylinder flow and to the data acquisition system. It may be observed in this figure that the utilization of a charge amplifier imposes oscillations, which are within the limits of the quantization noise (±0.25 bar/deg); whilst for the case of the current-to-voltage converter these oscillations

exceed the corresponding limits (±3.5×10-3 bar/deg). Therefore, it is possible to conclude that when a charge amplifier is used the effects of the noise generated by the data acquisition system predominate over the spurious component generated by in-cylinder flow, whilst in the case of the current-to-voltage converter this spurious component is the major responsible for the oscillations observed along the compression process.

The spectral distributions corresponding to the deviation curves shown in Figure 12a can be found in Figure 12b. These distributions characterize both the in-cylinder flow as well as the quantization error, as sources of white noise (random noise), having a considerable part of its spectral composition in the same frequency range occupied by the data of interest. Such behaviour makes it difficult to use low-pass filters or numerical smoothing without loss of useful signal, demanding especial care during the choice of the smoothing parameters, which vary with engine running condition (Zhong et al., 2004). Due to the high quantization noise in the data obtained with the charge amplifier, the remaining analysis of the experimental data composition was based on the current-to-voltage converter approach.

4.3 The combustion-driven spurious component

The ignition in diesel engines exhibits an eminently random character, being strongly influenced by the interaction of chemical and hydrodynamic phenomena occurring along the ignition delay (Maunoury et al., 2002). Because of this, a diesel engine operating in steady state presents cycle-to-cycle variations in the amount of fuel available for premixed combustion as well as in the locations where ignition occurs by first. In addition, the natural vibration modes of the gas contained in the cylinder are excited by the high burning rates that occur in the beginning of the combustion (Schmillen & Schneider, 1985), generating pressure oscillations of large amplitude that are rapidly dampened due to the high area/volume ratio of the cylinder cavity. Due to cycle-to-cycle combustion variability, different modes are excited in each cycle, causing the oscillations to vary in phase, characteristic frequencies and amplitude from one cycle to other.

Figure 13a shows the typical behavior of experimental pressure derivative data, where the cycle-to-cycle variability associated to the premixed combustion and to the following acoustic oscillations contrasts with the repeatability inherent to both the compression process and the diffusive combustion. In the periodograms presented in Figure 13b, the combustion-generated variability appears in the frequencies above 1000 Hz. This result is in accordance with the observations of Strahle (1977) and Strahle et al. (1977a, 1977b), who attributed the pressure data spectrum above 1000 Hz to the random phenomena associated to combustion.

In Figure 14a the deviation of the experimental data respective to the reference pressure derivative curve is shown along the combustion process for two cycles. As can be noticed, after 25 c.a. degrees the amplitude of the oscillations is dampened to a constant level slightly higher than that observed during compression, indicating that combustion amplifies the influence of the turbulence on experimental data. The spectral analysis of this deviation is shown in Figure 14b, where a periodic signal whose frequencies should correspond to the cylinder cavity characteristic frequencies can be seen (9.0 kHz for cycle 2; and 2.0, 6.0 and 11.0 kHz for cycle 13). Figure 14 confirms that the oscillations vary in phase, in characteristic frequencies and in amplitude from one cycle to other. This behavior may be used to remove the combustion-driven oscillations by data overlapping.

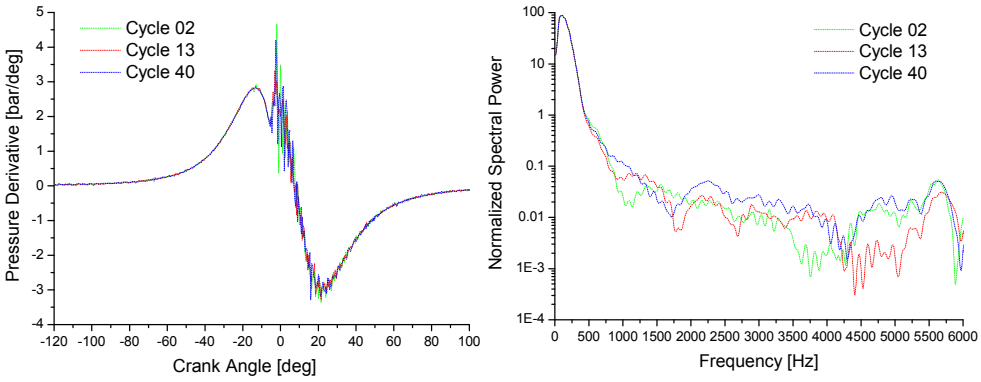

(a) (b)

Fig. 13. Pressure derivative experimental data and its spectral composition (D.I. diesel engine running at 2600 rpm and 80% of full load).

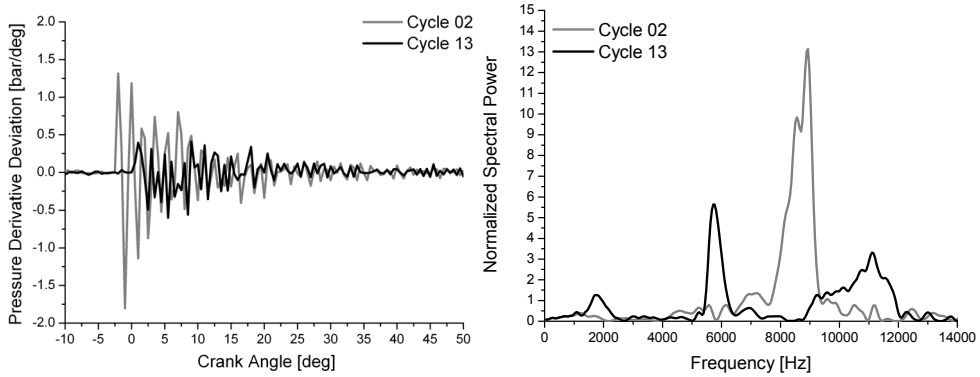

(a) (b)

Fig. 14. Combustion-driven spurious component of the experimental pressure derivative data (D.I. diesel engine running at 2600 rpm and 80% of full load).

4.4 Cycle-averaging as a data smoothing method

Cycle-averaging over a significant number of successive cycles is an effective method of data treatment, easing by overlapping the effects of cycle-to-cycle variations, combustion driven oscillations and measurement noise. This can be seen in Figure 15, which shows in its upper part the spectral composition of the spurious components of experimental data, whilst in its lower part the spectral composition of single-cycle pressure derivative data is compared to that of mean data (averaged over a sequence of 56 cycles). Data corresponding to cycles with the lowest noise level (13th cycle) and with the highest noise level (2nd cycle) are shown in the left and in the right parts of this figure, respectively.

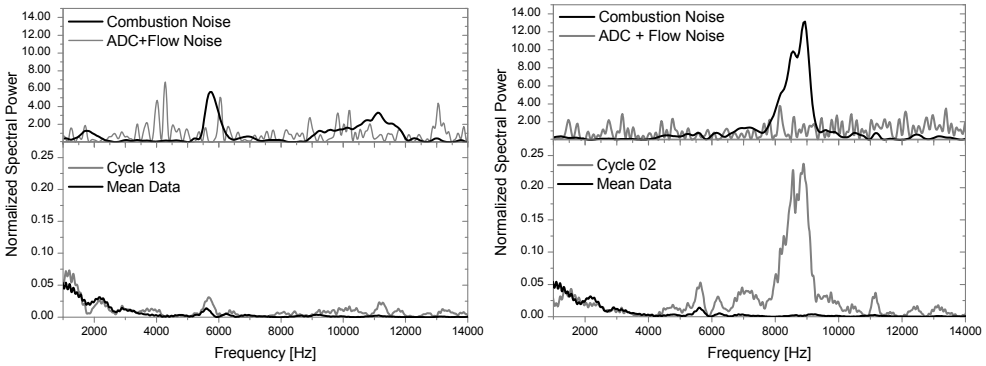

(a) (b)

Fig. 15. Noise in individual cycles and its reduction by cycle averaging (D.I. diesel engine running at 2600 rpm and 80% of full load).

Figures 16 and 17 show data of cylinder pressure and its derivative for the same engine operating conditions, where 95% confidence limits are displayed. Data of Figure 16 were obtained using a charge amplifier while for data of Figure 17 a current-to-voltage converter was used. In both cases data were averaged over a sequence of 56 cycles. Analyzing these figures it can be concluded that both transducer signal-conditioning procedures resulted in similar values for the cycle averaged cylinder pressure and its confidence limits, so that they are equivalent when the cylinder pressure is the parameter of interest. However, the studied procedures gave different results when evaluating pressure derivative, which is the data of greater interest for heat release analysis. The pressure derivative confidence interval obtained with the current-to-voltage converter was smaller than that obtained using the charge amplifier and subsequent numerical derivation, the former reaching only about 1/50 of the latter during most of the compression process as well as during late combustion.

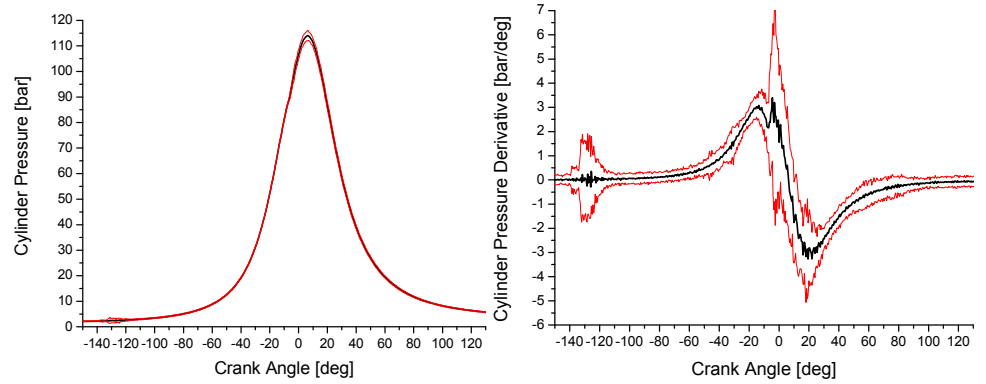

(a) (b)

Fig. 16. Indicating data obtained using a charge amplifier (D.I. diesel engine running at 2900 rpm and full load).

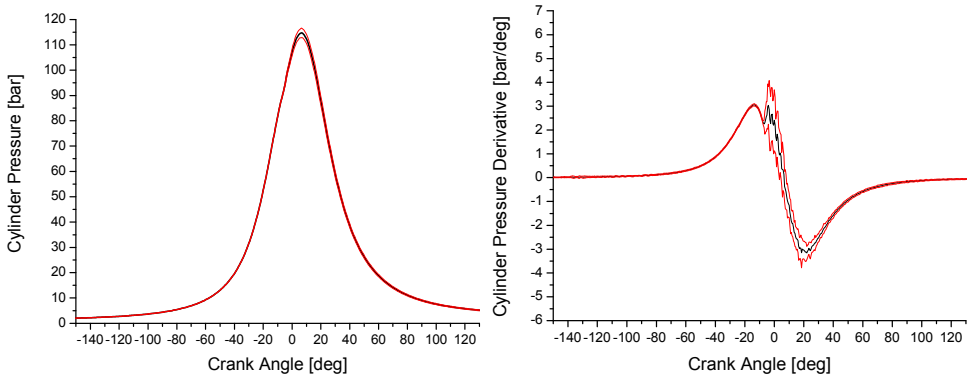

Fig. 17. Indicating data obtained using a current-to-voltage converter (D.I. diesel engine running at 2900 rpm and full load).

Considering the extension of the confidence intervals of pressure derivative data, it is expected that heat release results calculated from the charge amplifier data exhibit a more irregular and oscillatory pattern than those calculated from the current-to-voltage converter data. It is worth mentioning that large oscillations in the calculated heat release rate curve can result in negative values during the compression as well as during late combustion, which makes no physical sense. These oscillations make it difficult to determine the pressure data baseline, which in turn increases the uncertainty in the assessment of the burned fraction of fuel mass. Data shown in Figure 18a confirm that heat release curves

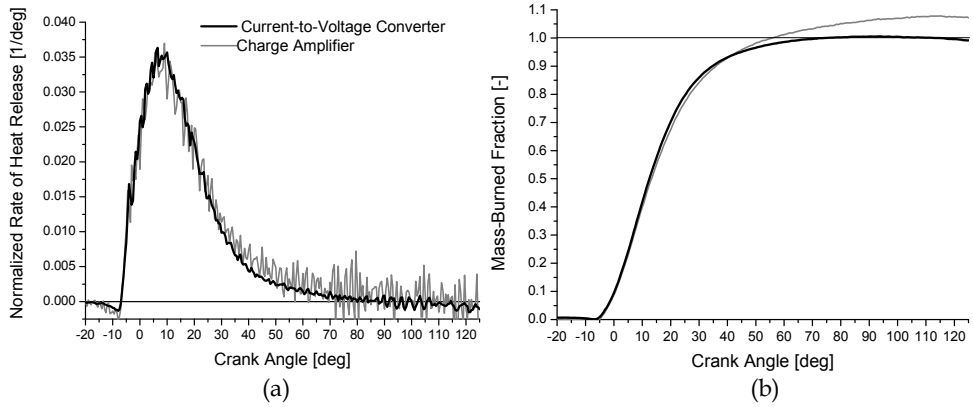

Fig. 18. Normalized heat release rate and fuel mass burned fraction (D.I. diesel engine running at 2900 rpm and full load).

calculated from charge amplifier data exhibit a higher noise level than those calculated from current-to-voltage converter data, while Figure 18b gives evidence of the differences in the calculated burned fraction of fuel mass, which are caused by this higher noise level.

5. References

Alwood, H. I. S.; Harrow, G. A. & Rose, L. J. (1970) A Multichannel Electronic Gating and Counting System for the Study of Cyclic Dispersion, Knock and Weak Mixture Combustion in Spark Ignition Engines. *SAE Paper 700063*.

Alyea, J. W. (1969) The Development and Evaluation of an Electronic Indicated Horsepower Meter. *SAE Paper 690181*.

Amann, A. C. (1985). Classical Combustion Diagnostics for Engine Research. *SAE Paper 850395*.

Benson, R. S. & Pick, R. (1974) Recent Advances in Internal Combustion Engine Instrumentation with Particular Reference to High-Speed Data Acquisition and Automated Test Bed. *SAE Paper 740695*.

Benson, R. S. & Whitehouse, N. D. (1983) *Internal Combustion Engines, 1st Ed.* Pergamon Press.

Brown, W. L. (1967) Methods for Evaluating Requirements and Errors in Cylinder Pressure Measurement. *SAE Paper 670008*.

Brown, W. L. (1973) The Caterpillar imep Meter and Engine Friction. *SAE Paper 730150*.

Bueno, A. V. ; Velásquez, J. A. & Milanez, L. F. (2009) A New Engine Indicating Measurement Procedure for Combustion Heat Release Analysis. *Applied Thermal Engineering*, Vol. 29, pp. 1657–1675.

Bueno, A. V. ; Velásquez, J. A. & Milanez, L. F. (2010) Heat Release and Engine Performance Effects of Soybean Oil Ethyl Ester Blending into Diesel Fuel. *Energy*, Vol. 36, pp. 3907-3916.

Bueno, A. V., Velásquez, J. A. & Milanez, L. F. (2011) Notes on 'A Methodology for Combustion Detection in Diesel Engines Through In-cylinder Pressure Derivative Signal'. *Mechanical Systems and Signal Processing*, Vol. 25, pp. 3209-3210.

Ding, Y. ; Stapersmal, D. ; Knoll, H. & Grimmelius, H. T. (2011) A New Method to Smooth the In-cylinder Pressure Signal for Combustion Analysis in Diesel Engines. *Proceedings of the Institution of Mechanical Engineers, Part A: Journal of Power and Energy*, Vol. 225, pp. 309-318.

Draper, S. C. & Li, T. Y. (1949) New High-Speed Indicator of Strain-Gauge Type. *Journal of Aerospacial Science*, Vol. 16, pp. 593-610.

Ficher, R. V. & Macey, J. P. (1975) Digital Data Acquisition with Emphasis on Measuring Pressure Synchronously with Crank Angle. *SAE Paper 750028*.

Franco, S. (2001) *Design with Operational Amplifiers and Analog Integrated Circuits, 3rd Ed*. McGraw-Hill.

Hountalas, D. T. & Anestis, A. (1998) Effect of Pressure Transducer Position on Measured Cylinder Pressure Diagram of High Speed Diesel Engines. *Energy Conversion and Management*, Vol 39, pp. 589-607.

Kistler (1956). *SLM Pressure Indicator*, DEMA Bull. 14.

Krieger, R. B. & Borman, G. L. (1966) The Computation of Apparent Heat Release for Internal Combustion Engines, *ASME paper 66-WA/DGP-4*.

Lancaster, D. R. ; Krieger, R. B. & Lienesch, J. H. (1975) Measurement and Analysis of Engine Pressure Data. *SAE Paper 750026*.

Lapuerta, M. ; Armas, O. & Bermúdez, V. (2000) Sensitivity of Diesel Engine Thermodynamic Cycle Calculation to Measurement Errors and Estimated Parameters. *Applied Thermal Engineering*, Vol. 20, pp. 843-861.

Lomb, N. R. (1976) Least-Squares Frequency Analysis of Unequally Spaced Data. *Astrophysics and Space Science*, Vol. 39, pp. 447-462.

Marzouk, M. & Watson, N. (1976) Some Problems in Diesel Engine Research with Special Reference to Computer Control and Data Acquisition. *Proceedings of the Institution of Mechanical Engineers*, Vol. 190, pp. 137-151.

Maunoury, B. ; Duverger, T. ; Mokaddem, K. & Lacas, F. (2002) Phenomenological Analysis of Injection, Auto-ignition and Combustion in a Small D.I. Diesel Engine. *SAE Paper 2002-01-1161*.

Payri, F. ; Olmeda, P. ; Guardiola, C. & Martín, J. (2011) Adaptive Determination of Cut-off Frequencies for Filtering the In-cylinder Pressure in Diesel Engines Combustion Analysis. *Applied Thermal Engineering*, Vol. 31, pp. 2869-2876.

Pinchon, P. (1984) Calage Thermodynamique du Point Mort Haut des Moteurs à Piston. *Revue de l'institut du Pétrole*, Vol 39(1).

Pischinger, R. & Glaser, J. (1985) Problems of Pressure Indication in Internal Combustion Engines. *Proceedings of COMODIA 1985*, Tokyo, Japan.

Randolph, A. L. (1990) Methods of Processing Cylinder-Pressure Transducer Signals to Maximize Data Accuracy. *SAE Paper 900170*.

Roth, K. J. ; Sobiesiak, A. ; Robertson, L. & Yates, S. (2001) In-Cylinder Pressure Measurements with Optical Fiber and Piezoelectric Transducers. *SAE Paper 2002-01-0745*.

Schmillen, K. & Schneider, M. (1985) Combustion Chamber Pressure Oscillations as a Source of Diesel Engine Noise. *Proceedings of COMODIA 1985*, Tokyo, Japan.

Stas, M. J. (1996) Thermodynamic Determination of T.D.C. in Piston Combustion Engines. *SAE Paper 960610*.

Strahle, W. C. (1977) Combustion Randomness and Diesel Engine Noise: Theory and Initial Experiments. *Combustion and Flame*, Vol. 28, pp. 279-290.

Strahle, W. C. ; Handley, J. C. & Varma, M. S. (1977a) Cetane Rating and Load Effects on Combustion Noise in Diesel Engines. *Combustion Science and Technology*, Vol. 17, pp. 51-61, 1977.

Strahle, W. C. ; Muthukrishnan, M. & Handley, J. C. (1977b) Turbulent Combustion and Diesel Engine Noise. *Proceedings of the Combustion Institute*, Vol. 16, pp. 337-346.

Teukolsky, S. A. ; Vetterling, W. T. & Flannery, B. P. (1966) *Numerical Recipes in C: The Art of Scientific Computing*. William H Press.

Wiebe, J. J. (1970) *Brennverlauf und Kreisprozes von Verbrennungsmotoren*, VEB-Verlag Technik Berlin, Germany.

Woschni, G. (1965) Computer Programs to Determine the Relationship between Pressure, Flow, Heat Release and Thermal Load in Diesel Engines. *SAE Paper 650450*.

Zhong, L. ; Henein, N. A. & Bryzik, W. (2004) Effect of Smoothing the Pressure Trace on the Interpretation of Experimental data for Combustion in Diesel Engines. *SAE Paper 2004-01-0931*.